




# Cost-Optimized Submarine Cables Using Massive Spatial Parallelism

Ronen Dar , Peter J. Winzer , A. R. Chraplyvy, Szilard Zsigmond, K.-Y. Huang ,  
Herve Fevrier, and Stephen Grubb

**Abstract**—We study the techno-economics of submarine systems constrained by a fixed electrical power supply. We show significant cost savings for high-capacity submarine systems using massive space-division multiplexing (SDM), even without assuming any savings from SDM-specific subsystem integration. Systems with about 100 parallel optical paths, e.g.,  $\sim 50$  fiber pairs are shown to provide minimum cost/bit, operating at reduced spectral efficiencies and deep within the linear regime. While advanced nonlinearity-optimized fibers and digital nonlinearity compensation schemes provide little to no gain in such systems, SDM integration of amplifiers and transponders is shown to be a source for significant additional cost savings. We further examine the permissible cost premium for multicore fibers in such massively parallel systems and revisit various design tradeoffs for optical amplifiers, showing that a reduced noise figure can be traded for better power conversion efficiency. We also evaluate potential gains from increasing the available electrical supply power and discuss reliability aspects of massively parallel submarine systems.

**Index Terms**—Capacity, cost, space-division multiplexing, submarine.

## I. INTRODUCTION

IN CONTRAST to terrestrial optical fiber systems, the capacity of modern submarine links with up to 8 fiber pairs [1] is starting to be limited by the maximum electrical power that can be fed into the submarine cable to supply its inline optical amplifiers (OAs) [2]–[5]. Various strategies to overcome this capacity limit have been proposed, including (i) power-constrained optimization of OA spacings [2], [3], [6], (ii) trading logarithmic for linear capacity gains by shifting systems towards linear operation while increasing their spatial multiplicity [4], [7]–[12], (iii) trading reduced OA bandwidths for increased OA efficiencies [13], [14], and (iv) using power-efficient probabilistically shaped modulation and digital nonlinearity compensation (NLC) [15], with partially contradicting conclusions depending on the optimization criteria.

Manuscript received May 16, 2018; accepted May 21, 2018. Date of publication May 30, 2018; date of current version July 19, 2018. (Corresponding author: Ronen Dar.)

R. Dar, P. J. Winzer, and A. R. Chraplyvy are with Nokia Bell Labs, Holmdel, NJ 07733 USA (e-mail: ronen.dar@nokia-bell-labs.com; peter.winzer@nokia-bell-labs.com; andrew.chraplyvy@nokia-bell-labs.com).

S. Zsigmond and K.-Y. Huang are with Nokia Corporation, Murray Hill, NJ 07974 USA (e-mail: szilard.zsigmond@nokia.com; k-y.huang@nokia.com).

H. Fevrier and S. Grubb are with Facebook Inc., Menlo Park, CA 94025 USA (e-mail: hervef@fb.com; sgrubb@fb.com).

Color versions of one or more of the figures in this paper are available online at <http://ieeexplore.ieee.org>.

Digital Object Identifier 10.1109/JLT.2018.2841810

Here, we consider the *overall system cost/bit* as a techno-economically more conclusive optimization metric than the system's cable capacity or energy consumption. This puts cable capacity in relation to the aggregate cost of cable, fiber, repeaters, transponders, and marine deployment. Extending the results of Ref. [16] and refining the calculations presented there by additionally accounting for the effect of OA noise accumulation, we show that *cost/bit-optimized* submarine cables obey significantly different design rules from *capacity-optimized* cables.

Our key findings include:

- Cost-optimized systems favor massive space-division multiplexing (SDM) with  $\sim 100$  parallel paths (i.e.,  $\sim 50$  parallel paths per direction or  $\sim 50$  fiber pairs)
- These systems use relatively long repeater spans of around 90 km.
- These systems save about 40% in cost/bit compared to the state-of-the-art, while having 5x higher cable capacity.
- In line with Refs. [13], [14], using less bandwidth per spatial path is beneficial if this increases the power-efficiency of optical amplification.
- A better power efficiency of optical amplifiers may be traded for a higher noise figure (NF) in a cost-optimized system.
- Since cost-optimized systems operate deep in the linear regime, NLC provides little to no benefit, nor do low-nonlinearity fiber designs reduce the overall system cost/bit.
- Even if the electrical supply power was increased beyond state-of-the-art levels, the overall system cost/bit would not drop significantly, favoring multiple parallel cables as opposed to even higher-capacity designs.

It is important to note that the above key conclusions are reached by using massively parallel arrays of *state-of-the-art* components and subsystems, *without* having to invoke any SDM-specific technologies and their associated cost savings from array integration. In fact, we show that even for a significant *cost premium*, multi-core fiber (MCF) based on standard single-mode cores can yield overall lower-cost systems compared to massive bundles of advanced fiber. On the other hand, we show that very significant gains are expected on top of the above benefits from array integration of amplifiers and transponders. It is therefore well imaginable that future submarine systems will first leverage massively parallel state-of-the-art components to reduce their cost/bit, before extracting further cost savings by gradually migrating to integrated array

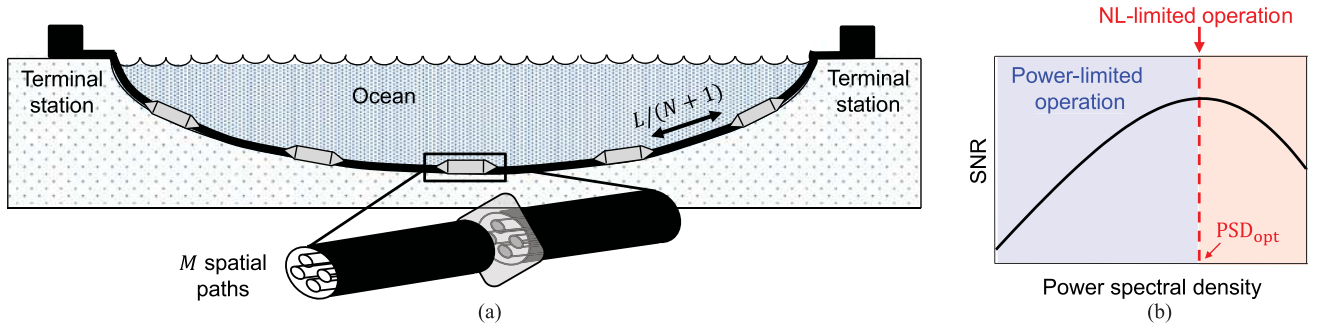


Fig. 1. (a) Submarine system model. (b) SNR versus power spectral density; a submarine system is limited by the available supply power feed when  $\text{PSD}_{\text{max}} < \text{PSD}_{\text{opt}}$  and by fiber nonlinearities when  $\text{PSD}_{\text{max}} \geq \text{PSD}_{\text{opt}}$ . Optimized systems never operate beyond  $\text{PSD}_{\text{opt}}$ .

solutions as the respective arrayed subsystems start to become available.

## II. SUBMARINE SYSTEM MODEL

We consider submarine cables containing  $M$  parallel spatial paths (i.e.,  $M/2$  fiber pairs) and  $N$  uniformly spaced OAs per optical path, with a system bandwidth  $B$ , cf. Fig. 1(a). We define the total cable capacity  $C$  across all  $M$  spatial paths (and summing up the capacity in *both propagating directions*) as<sup>1</sup> [17]

$$C = 2MB \log_2(1 + \text{SNR}), \quad (1)$$

where the signal-to-noise ratio (SNR) is given by (see Appendix)

$$\text{SNR} = \frac{\text{PSD}_{\text{sig}}}{Nh f \left( F e^{\frac{\alpha L}{N+1}} - 1 \right) + \chi' \log(B) \text{PSD}_{\text{sig}}^3}, \quad (2)$$

with  $\text{PSD}_{\text{sig}}$  being the power spectral density of the transmitted signal. We develop our formalism in terms of PSD instead of per-channel launch powers (*i*) to reflect the fact that modern high-spectral-efficiency systems operate with very narrow gaps between their spectrally flat per-channel signal spectra, and (*ii*) to use the overall system bandwidth  $B$  as opposed to the combination of channel bandwidth and number of channels as a single design parameter. This neglects symbol-rate-dependent variations in nonlinear transmission performance [18]–[20], which, however, are insignificant here, as we assume perfect Gaussian modulation and no NLC, in which case the NLIN coefficient is symbol-rate independent [20]. In addition, since cost optimized submarine systems will be shown to operate in the linear regime, small performance differences arising from nonlinearity considerations are irrelevant to this study.

The first term in the denominator on the right hand side of Eq. (2) represents the power spectral density of the ASE, with  $hf$  corresponding to the photon energy at the carrier frequency  $f$ ,  $F$  denoting the OAs' NF,  $L$  the length of the cable, and  $\alpha$  the fiber loss coefficient. The second term in the denominator on the right hand side of Eq. (2) corresponds to the power spectral density of the NLIN induced by fiber Kerr nonlinearity. It assumes a first-order perturbation analysis and excludes ASE

induced nonlinear distortions, two assumptions that are well justified in the scenarios considered throughout this paper [21], [22]. We write the NLIN coefficient as  $\chi' \log(B)$  to indicate the logarithmic scaling of NLIN with  $B$  [23]–[25], as detailed in the Appendix, and extract  $\chi'$  from the NLIN Wizard [26], [27]. The AIR expression in Eq. (1) implicitly assumes ideal coding and Gaussian modulation, which can be achieved, e.g., using probabilistic shaping methods such as those presented in Refs. [28]–[31]. The AIR expression also assumes that NLIN is non-removable, additive white Gaussian noise (AWGN); note though that this assumption has little impact on the main outcomes of this paper, as we will show that cost-optimized submarine systems operate in a power-limited regime where the signal power is too low to produce significant nonlinear distortions. Finally, we note that the SNR expression may further be multiplied by an SNR degradation factor  $\delta \leq 1$  if one desires to account for implementation penalties. In this paper we do not include such factors, except for some analyses performed in Sec. IV, where we show that for  $\delta$  as large as 3 dB only insignificant changes in the general, high-level conclusions of our work are obtained.

We assume a fixed electrical supply power feed of  $P_e$  to the entire cable. The maximum available PSD that can be launched into each optical path can therefore be deduced from the following inequality

$$MB \sum_{i=1}^N \left[ \text{PSD}_{\text{in}}^{(i)} (G - 1) + \text{PSD}_{\text{ASE}} \right] \leq \eta_{oe} P_e. \quad (3)$$

The right hand side of this inequality represents the maximum available optical power within the cable, given by [3]

$$\eta_{oe} P_e = \eta_{oe} \frac{\Delta V^2}{4RL}, \quad (4)$$

where  $\eta_{oe} < 1$  represents the OAs' wallplug efficiency (i.e., the ratio between the optical output power and the electrical input power),  $R$  is the cable's ohmic resistance, and  $\Delta V$  is the supply voltage drop across the cable, using either a single-sided or a double-sided feed [4], [32]. Throughout this paper we consider 11,000-km Trans-Pacific and 6,000-km Trans-Atlantic cables. We assume the Trans-Atlantic cable to use a 15-kV supply (enabling uninterrupted operation in case of a cable short), and the Trans-Pacific cable to use a 30-kV supply ( $\pm 15$ kV on both ends to maximize capacity without resilience to a cable short [32]). The impact of changing supply power levels is studied further in Section VI-B. System parameters are listed in Table I.

<sup>1</sup>Strictly speaking, since we treat fiber nonlinearities as an equivalent additive white Gaussian noise, Eq. (1) is not the system's information capacity but rather an achievable information rate (AIR).

TABLE I  
CABLE PARAMETERS

	Trans-Atlantic	Trans-Pacific
Length $L$	6,000 km	11,000 km
Resistance $R$	1 $\Omega$ /km	1 $\Omega$ /km
Supply voltage drop $\Delta V$	15 kV	30 kV
OA efficiency $\eta_{oe}$	2.5%	2.5%
Maximum power supply $\eta_{oe}P_e$	234 W (54 dBm)	511 W (57 dBm)
OA bandwidth $B$	4.3 THz	4.3 THz
Noise figure $F$	5 dB	5 dB

The left hand side of Eq. (3) corresponds to the overall optical power produced within the submarine cable. The  $i$ -th term in the summation corresponds to the optical power produced by the  $i$ -th OA in each spatial path, where  $G = e^{\alpha L/(N+1)}$  is the OA gain,  $\text{PSD}_{\text{ASE}} = hf(FG - 1)$  is the PSD of the injected ASE, and  $\text{PSD}_{\text{in}}^{(i)} = (\text{PSD}_{\text{sig}} + (i-1)\text{PSD}_{\text{ASE}})/G$  is the PSD of the optical signal plus any previously accumulated ASE at the input to the  $i$ -th OA. By substituting these into Eq. (3) we find that the PSD of the signal launched into each spatial path is upper-bounded by

$$\begin{aligned} \text{PSD}_{\text{sig}} &\leq \text{PSD}_{\text{max}} \\ &= \frac{\eta_{oe}P_e}{NMB} \frac{G}{G-1} - \text{PSD}_{\text{ASE}} \left( \frac{N+1}{2} + \frac{1}{G-1} \right). \end{aligned} \quad (5)$$

Note that this upper bound reduces to

$$\text{PSD}_{\text{max}} \simeq \frac{\eta_{oe}P_e}{NMB}, \quad (6)$$

when  $G \gg 1$  and  $\eta_{oe}P_e/(NMB) \gg \text{PSD}_{\text{ASE}}(N+1)/2$ ; these conditions are typically met in cost-optimized systems with less than  $\sim 500$  spatial paths. The upper bound, Eq.(6), was used in Ref. [16] to derive similar conclusions to the ones presented in this paper.

Besides the maximum available supply power feed, cable capacity may also be limited by fiber nonlinearities (NL). The NL-optimized PSD is given by [33]

$$\text{PSD}_{\text{opt}} = \left[ \frac{Nhf(Fe^{\alpha L/(N+1)} - 1)}{2\chi' \log(B)} \right]^{1/3}. \quad (7)$$

An optimized system will either operate at  $\text{PSD}_{\text{max}}$  or at  $\text{PSD}_{\text{opt}}$ , whichever is smaller. As illustrated in Fig. 1(b), the first case refers to systems operating in the linear, power-limited regime, whereas the latter case refers to systems that operate in the NL-limited regime. Optimized systems never operate beyond  $\text{P}_{\text{opt}}$  (red shaded area).

### III. SUBMARINE COST MODEL

Throughout this paper we consider a cost model that accounts for

- Marine survey and deployment cost ( $C_D$ )

TABLE II  
SYSTEM COST PARAMETERS (NORMALIZED TO TRANSPONDER COST PER 100G)

Deployment per km ( $c_D$ )	0.7
Cable per km ( $c_C$ )	0.5
Fiber per km ( $c_F$ ) (assuming PSCF110)	0.005
Optical amplifier ( $c_{OA}$ )	2
Transponder per 100G ( $c_T$ )	1

- Cable cost without fiber ( $C_C$ )
- Fiber cost ( $C_F$ )
- Optical amplifier cost ( $C_{OA}$ )
- Transponder cost ( $C_T$ )

We assume that deployment, cable and fiber costs are proportional to the length of the system, i.e.,  $C_D = c_D L$ ,  $C_C = c_C L$  and  $C_F = c_F L$ . The impact of a potential cost premium for massively parallel SDM systems is discussed in Section V. The total cost of OAs is given by  $C_{OA} = c_{OA} NM$  with  $c_{OA}$  representing the cost of a single OA; possible fixed costs of repeater bottles housing a varying number of OAs are assumed to be negligible and are not considered here. The overall cost of transponders is given by  $C_T = c_T C$ . Potential cost savings from high-volume discounts which may be applicable for massively parallel systems, as well as potential cost savings from the ability to design cheaper, lower-complexity transceivers for systems operating at a comparatively low spectral efficiency (SE) in the linear regime are discussed in Section VII. All of the above costs sum up to a *total system cost* of

$$C_{\text{tot}} = (c_D + c_C + c_F M)L + c_{OA} NM + c_T C. \quad (8)$$

Table II lists the relative cost numbers that we use throughout the paper, assuming state-of-the-art technology and C-band, including C-band OAs. Due to cost confidentiality reasons, all numbers are normalized to the cost per 100 G of an advanced coherent optical transponder.

### IV. COST/BIT AND CAPACITY OPTIMIZATIONS

In this section we focus on the optimization of span length  $L/(N+1)$  and number of spatial paths  $M$ . We consider throughout this section submarine cables with strands of pure silica core fiber with an effective area of  $110 \mu\text{m}^2$  (PSCF110), a nonlinearity coefficient of  $\gamma = 0.81 \text{ W/km}$ , a loss coefficient of  $\alpha = 0.16 \text{ dB/km}$ , and a chromatic dispersion (CD) coefficient of  $D = 18 \text{ ps/km}\cdot\text{nm}$ .

#### A. Optimum Span Lengths

Figs. 2(a) and (b) show the cable capacity  $C$  (aggregate over both directions, blue, left y-axis) and the normalized cost/bit (red, right y-axis) as a function of span length for Trans-Pacific and Trans-Atlantic systems, respectively, using  $M = 16$  spatial paths (8 fiber pairs). Capacity optimization yields significantly different span lengths than when optimizing for cost/bit: While a capacity-optimized system operates at nonlinearly-optimized



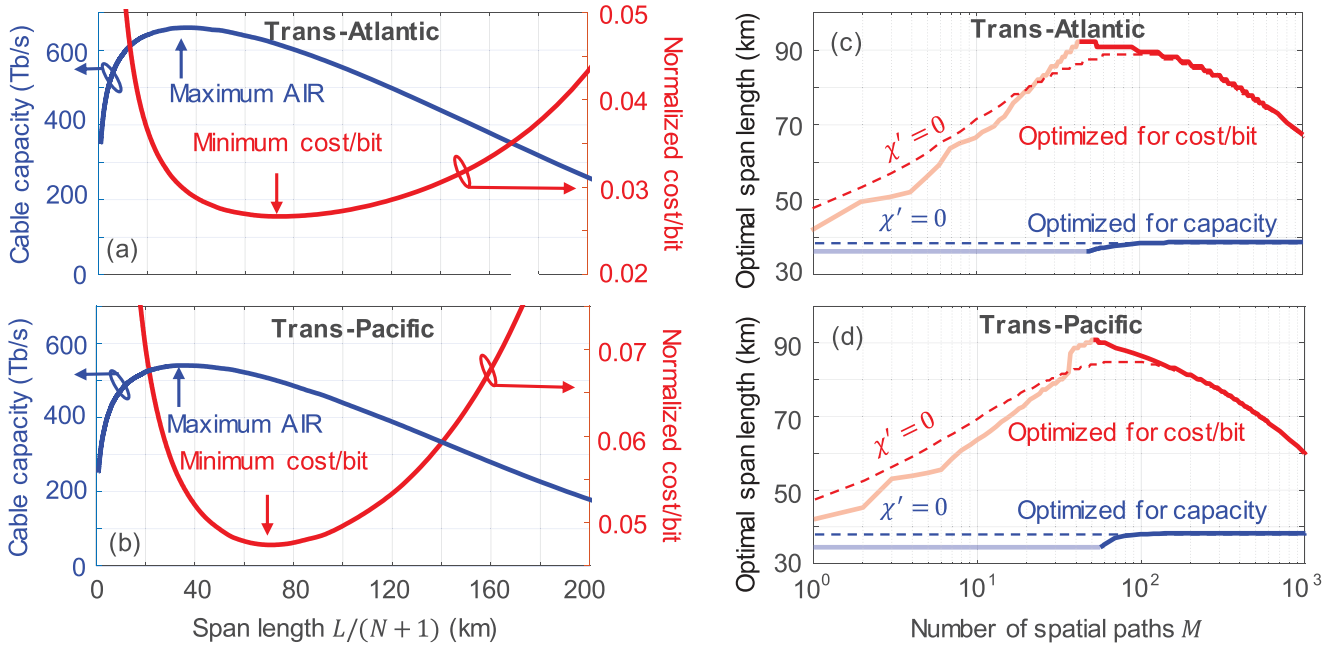


Fig. 2. (a-b) Cable capacity (aggregate over both directions, left) and normalized cost/bit (right) for submarine systems using 16 PSCF110 strands (8 fiber pairs). (c-d) Optimal span length for capacity- and cost/bit-optimized systems. Dashed curves assume  $\chi' = 0$  (nonlinearity-free systems); light and dark colors indicate NL- and power-limited regimes, respectively.

spans of 35 km, a cost-optimized system uses 70-km spans. The cost-optimized system for this parameter set is  $\sim 12\%$  cheaper than the capacity-optimized system. The difference gets larger as the spatial multiplicity  $M$  is increased, cf. Fig. 2(c) and (d), showing the optimal span length versus the number of parallel spatial paths when optimizing for cost/bit (red) or cable capacity (blue). Light colors indicate regimes limited by fiber nonlinearity (operating at  $\text{PSD}_{\text{opt}} < \text{PSD}_{\text{max}}$ ), while dark colors indicate electrical supply power limitations (operating at  $\text{PSD}_{\text{max}}$ ). The fact that  $M$  is an integer number gives the red solid curves a somewhat jittery look. For the assumed parameters, cost/bit-optimized systems are NL-limited ( $\text{PSD}_{\text{max}} > \text{PSD}_{\text{opt}}$ ) up to  $M \sim 50$  spatial paths (e.g.,  $\sim 25$  fiber pairs). Dashed lines additionally show the nonlinearity-free results, obtained by setting  $\chi' = 0$ . This corresponds to a lower bound that represents fibers with negligible nonlinear distortions or completely idealized digital nonlinearity compensation. Clearly, for Trans-Atlantic systems, capacity-optimized systems with more than  $M \sim 70$  spatial paths operate well within the linear regime whereas cost-optimized systems require approximately  $M \sim 100$  spatial paths to get into the linear regime of operation. For Trans-Pacific systems, both cost-optimized and capacity-optimized systems operate in the linear regime once  $M$  exceeds  $\sim 100$  (or  $\sim 50$  parallel paths per direction).

### B. Optimum Number of Parallel Spatial Paths

Figs. 3(a) and (b) show the normalized cost/bit versus  $M$  for cost-optimized systems. Interestingly, the lowest-cost system uses as many as  $\sim 100$  parallel paths (50 paths per direction), which can be any mixture of parallel fibers, cores of MCFs, or modes of few-mode cores, assuming comparable system perfor-

mance over such waveguides/modes; a significant cost reduction of 34% and 44% compared to current cables that contain only  $M = 16$  parallel paths is found for Trans-Atlantic and Trans-Pacific systems, respectively. As shown in Figs. 3(c) and (d), the cable capacities (blue, left y-axes) of such systems are increased by a factor of  $\sim 5$  without increasing the electrical supply power; the systems operate at only a modest spectral efficiency reduction (SE, red, right y-axis) of  $\sim 20\%$  per spatial path compared to  $M = 16$  paths. Optimizing for system cost/bit yields SEs of  $6 \sim 7$  b/s/Hz, which is significantly higher than the SE of  $\sim 3$  b/s/Hz derived for capacity-optimized systems [9]. Dashed lines, again, represent nonlinearity-free results ( $\chi' = 0$ ). Clearly, cost/bit-optimized systems operate within the linear regime. At a first glance counter-intuitively, NLC will therefore be of little to no value in such cost-optimized submarine systems.

Figs. 3(e) and (f) show a more detailed cost break-down versus  $M$ ; for the cost-optimized system with  $\sim 100$  parallel paths, the fixed costs of cable and deployment, as well as the cost of fiber are about equal and noticeably below the costs of OAs and transponders. These results have important implications on the choice of fibers and the design of optical amplifiers for submarine systems, as discussed further in Sections V and VI.

### C. Implementation Penalties

In Fig. 4 we compare the optimal span length and the normalized cost/bit of cost-optimized Trans-Atlantic and Trans-Pacific systems with no implementation penalty (red curves, extracted from Figs. 2(c), 2(d), 3(a) and 3(b) with the results for a 3-dB implementation penalty ( $\delta$ ), representing a performance gap from the theoretical Shannon capacity (blue curves). These are obtained by dividing the SNR term in Eq. (1) by  $\delta$ . The

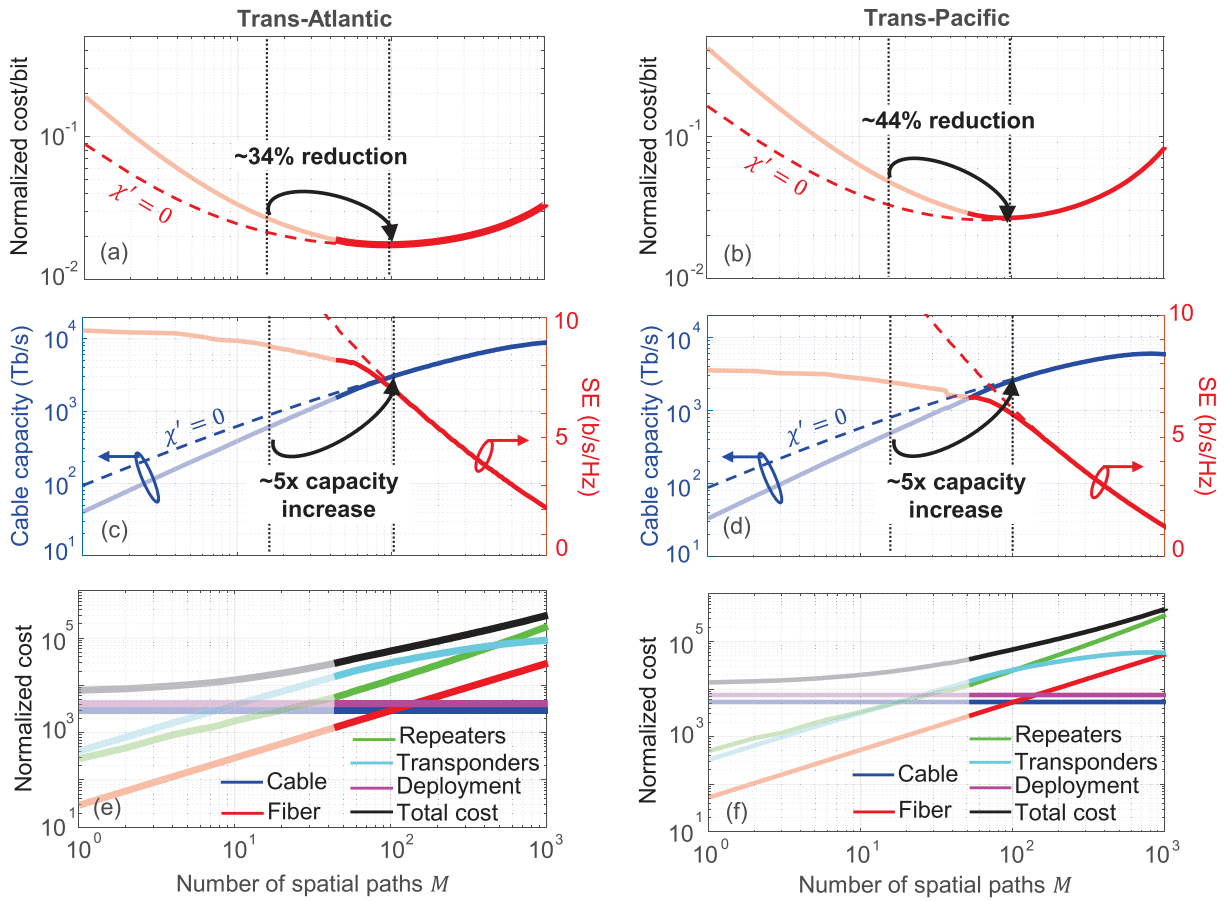


Fig. 3. (a–b) Normalized cost/bit, (c–d) cable capacity (aggregate over both directions) and SE, and (e–f) breakdown of the overall system cost versus number of spatial paths. Dashed curves assume  $\chi' = 0$  (nonlinearity-free systems). Light and dark colors indicate NL- and power-limited regimes, respectively.

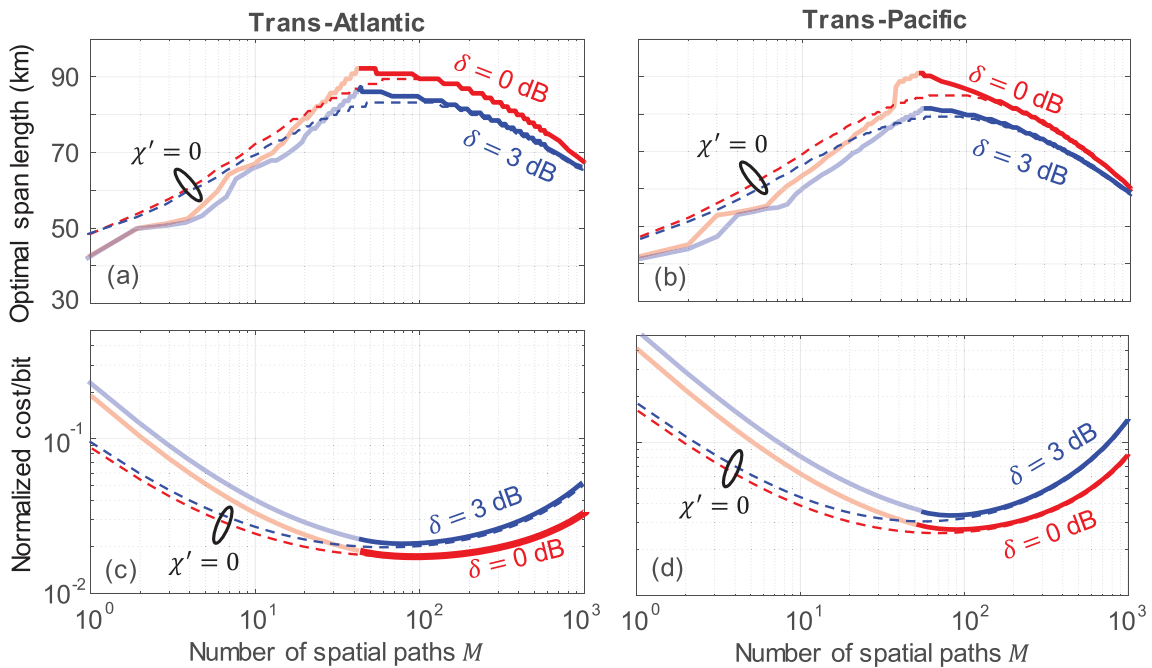


Fig. 4. (a–b) Optimal span length and (c–d) normalized cost/bit versus number of spatial paths for cost-optimized Trans-Atlantic and Trans-Pacific systems using PSCF110. Red: no implementation penalty ( $\delta = 0$ ); blue: implementation penalty of  $\delta = 3$  dB. Light and dark colors indicate NL- and power-limited regimes of operation. Dashed curves assume  $\chi = 0$  (nonlinearity-free systems).

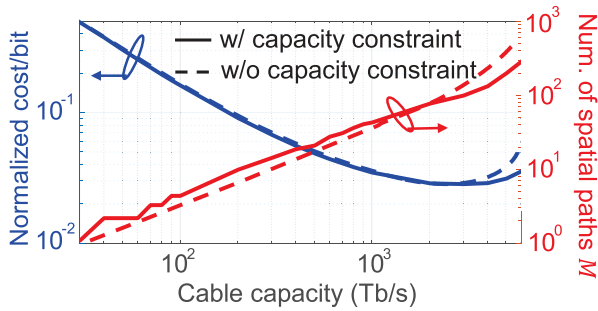


Fig. 5. Normalized cost/bit (blue, left axis) and corresponding number of spatial paths (red, right axis) versus cable capacity (aggregate over both directions) for Trans-Pacific PSCF110 systems with optimized span lengths. Dashed curves are extracted from Figs. 3(b) and (d). Solid curves correspond to optimized systems whose specified cable capacity is given by the x-axis.

two cases behave quite similarly, with the optimal span length being slightly shorter and the cost/bit slightly higher in the presence of an implementation penalty. Our important finding of cost-optimized submarine cables favoring  $\sim 100$  parallel spatial paths is not changed by the assumption of an implementation penalty, however.

#### D. Systems With Fixed Cable Capacity

All the results above were obtained by minimizing the cost/bit of a cable for a given number of spatial paths, but without employing any constraint on the resulting cable capacity. In Fig. 5 we take a different approach: We examine power-constrained submarine cables that are also designed for a given overall cable capacity and optimize both span length and number of spatial paths for these cables. Solid curves show the optimum normalized cost/bit and the corresponding number of spatial paths versus the specified cable capacity (aggregate over both directions) for Trans-Pacific cables. For comparison, we extract from Figs. 3(b) and (d) the normalized cost/bit for cost-optimized and capacity-unconstrained Trans-Pacific systems and plot them as a function of the resulting cable capacity (dashed). The results are about the same in both cases, both for the normalized system cost/bit and for the corresponding number of spatial paths. Cables with specified capacities higher than 2 Pb/s favor massively parallel solutions with more than 100 spatial paths.

#### V. FIBER TYPES AND MULTI-CORE TECHNOLOGY

To examine the impact of fiber types on system cost, we plot in Fig. 6 the normalized cost/bit vs. the number of spatial paths in a Trans-Pacific system with cost-optimized span lengths, considering standard single-mode fibers (SSMFs) as well as nonlinearity-tolerant PSCFs with various core areas. Table III details the parameters assumed for the various fiber types as well as the optimum cost/bit with the corresponding number of spatial paths and cable capacities. Owing to its higher loss, the use of SSMF makes the overall system cost/bit  $\sim 10\%$  more expensive compared to the best cost/bit attained with PSCF110. Importantly, though, the lower-nonlinearity (but higher-cost) PSCF130 and PSCF150 yield *higher-cost/bit* systems compared to PSCF110, as the better nonlinear tolerance of these fibers is

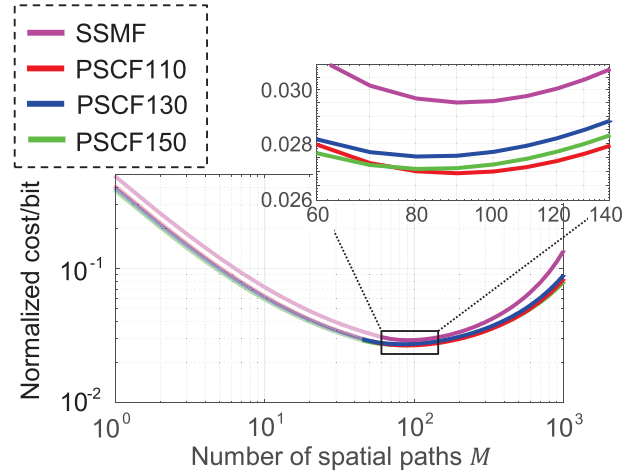


Fig. 6. Normalized cost/bit versus number of spatial paths for Trans-Pacific systems using PSCF110 (red), PSCF130 (blue), PSCF150 (green), and SSMF (magenta). Light and dark colors indicate NL- and power-limited regimes of operation.

TABLE III  
FIBER PARAMETERS AND OPTIMUM SYSTEM COST/BIT

	SSMF	PSCF110	PSCF130	PSCF150
Loss (dB/km)	0.185	0.160	0.162	0.154
CD (ps/km/nm)	18	20.5	20.5	20.8
Effective area ( $\mu\text{m}^2$ )	80	110	130	150
NL coef. (1/W/km)	1.31	0.81	0.68	0.59
Fiber cost ratio	1	6	7.5	10
Normalized cost/bit	0.0295	0.0269	0.0275	0.0271
Optimum $M$	90	90	90	90
Capacity $C$ (Tb/s)	2,046	2,410	2,450	2,560

not important in systems operating in the (supply power limited) linear regime.

Owing to the high fiber count of cost-optimized systems, state-of-the-art cabling technologies or marine deployment procedures may no longer be adequate, and cables supporting  $\sim 100$  strands of fiber may come at a cost premium. To avoid higher fiber count cables, *multi-core fiber technology* [34] is a potential solution to keep the number of fiber pairs low while yielding the desired large number of parallel spatial paths; MCFs may come at a per-core cost premium relative to single-core fiber, though. To analyze these two potential cost premiums, Fig. 7 shows the optimized cost/bit and the corresponding number of spatial paths as a function of the cost premium for cables that can support a high number of PSCF110 (blue curves), as well as for standard cabling technology with MCFs based on cheaper SSMF core technology (red curves). That is, in the first case we assume a cost premium  $p$  on the cable (i.e.,  $c_C \rightarrow p c_C$ ) whereas in the latter case we assume a cost premium per MCF core (i.e.,  $c_F \rightarrow p c_F$ ). For example, a PSCF110-based system with a 4x cable cost premium is more expensive than an MCF-based systems as long as the MCF cost premium per core is smaller than 10x. This is mainly due to the larger significance of cable cost

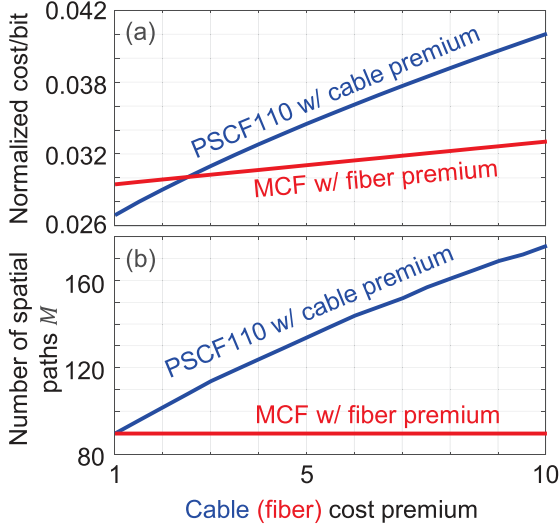


Fig. 7. (a) Normalized cost/bit and (b) the corresponding number of spatial paths versus cable and MCF cost premium for Trans-Pacific systems with optimized span lengths and numbers of spatial paths. Blue curves consider PSCF110-based solutions with a cost premium on the *cable only*; red curves consider MCF-based solutions based on SSMF core technologies, with a cost premium on the *fibers only*.

compared to fiber cost in the overall cost of the system, cf. Fig. 3(f). Importantly, note that the number of spatial paths required for optimized MCF-based systems is relatively constant with respect to the fiber cost premium, while it grows monotonically with cable cost premium for optimized PSCF110-based systems due to the need to amortize the higher cable cost among more fibers.

## VI. OPTICAL AMPLIFIERS

Driving submarine systems deep into the linear regime of operation has important implications on the design of optical amplifiers as well. In this section we examine the tradeoff between amplifier efficiency and NF, as well as the system implications of optical amplifier bandwidths [13], [14].

### A. Optical Amplifier Efficiency and Noise Figure

Following Eqs. (1), (2), and (7), in the NL-limited regime of operation, cable capacity is limited by  $\text{PSD}_{\text{opt}}$  and is given by

$$C = 2MB \log_2 \left( 1 + \frac{2 [Nhf(Fe^{\alpha L/(N+1)} - 1)]^{-\frac{2}{3}}}{3 [2\chi' \log(B)]^{\frac{1}{3}}} \right), \quad (9)$$

Evidently, the optical amplifiers' NF affects the cable capacity per complex degree of freedom roughly as  $2/3 \log_2 F$  (assuming operation in the high-SNR regime which is typically the case in NL-limited systems), i.e., a 3-dB increase in the amplifier NF reduces the achievable SE per complex degree of freedom by about  $2/3$  bits/s/Hz. In the power-limited regime of operation, however, we have

$$C \simeq 2MB \log_2 \left( 1 + \frac{1}{MBN^2 h f e^{\alpha L/(N+1)} \frac{\eta_{oe} P_e}{F}} \right), \quad (10)$$

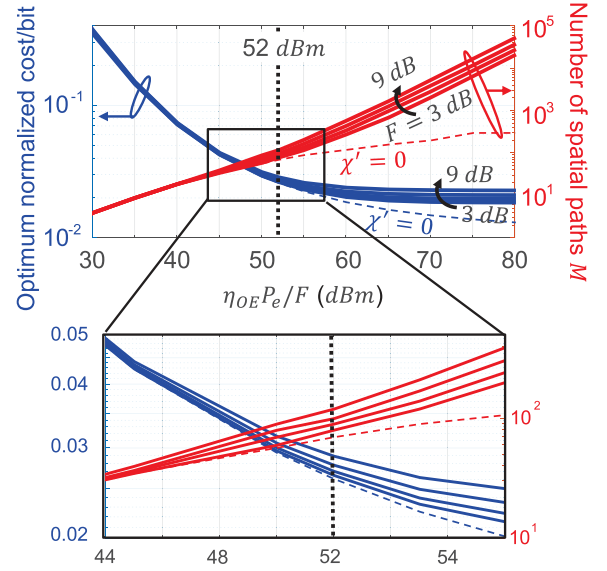


Fig. 8. Optimum cost/bit (left) and number of parallel spatial paths per cable (right) for Trans-Pacific PSCF110 systems, versus ratio of optical supply power ( $\eta_{oe} P_e$ ) to amplifier noise figure ( $F$ ).

assuming  $\text{PSD}_{\text{max}} \simeq \eta_{oe} P_e / (MNB)$ , which is satisfied for most relevant regimes of operations, and  $F e^{\frac{\alpha L}{N+1}} \gg 1$ , which holds true in systems with fiber spans longer than  $\sim 30$  km. While we see from Eq. (10) that the system now enters the capacity as  $F^{-1}$  into the capacity, i.e., a 3-dB increase in NF reduces the achievable SE by about 1 bits/s/Hz, we also see the new possibility of *trading NF for OA efficiency*. That is, OAs with increased power efficiency may represent a preferred solution even if they have worse NFs, as long as the ratio  $\eta_{oe}/F$  improves; this may open up possibilities for new submarine OA designs and even allow for semiconductor optical amplifiers (SOAs) to be considered in submarine links, as these hold the promise of significantly higher wallplug efficiencies [35], while having only slightly higher NFs. Note in this context that SOA based coherent optical fiber transmission systems have recently been demonstrated [36].

To quantify the trade-off between optical amplifier NF and energy efficiency on submarine system costs, Fig. 8 shows the minimum cost/bit (left) with optimized  $M$  and  $N$ , as in previous sections, and the corresponding optimum  $M$  (right) as a function of  $\eta_{oe} P_e / F$  for various NFs ranging from 3 dB to 9 dB. The dashed curves assume  $\chi' = 0$ , letting the small dependence on  $F$  vanish. For small values of  $\eta_{oe} P_e / F$ , cable capacity is limited predominantly by the low available supply power, and optimized systems operate deep in the linear regime where the cost/bit and the number of spatial paths only leads to a small explicit dependence on  $F$  for a given ratio  $\eta_{oe} P_e / F$ . With increased values of  $\eta_{oe} P_e / F$ , cost-optimized systems employ an increasing number of spatial paths in order to keep the per-channel launch power sufficiently low and keep the system in the cost/bit-optimized linear regime of operation. At high levels of  $\eta_{oe} P_e / F$ , the system starts to become nonlinear because diluting the optical power among even more spatial paths



is no longer cost effective; in this regime, the difference between the various NF-curves become more notable and so is the difference between the dashed and solid curves, implying that fiber nonlinearity becomes more important and the linearized Eq. (10) becomes less accurate. At  $\eta_{oe}P_e/F = 52$  dBm, which corresponds to the OA power supply and NF values assumed in previous sections, we observe  $\sim 10\%$  change in optimized cost/bit when the NF changes from 3 dB to 9 dB.

### B. Electrical Supply Power

In addition, Fig. 8 also illustrates the potential cost savings from increasing the available supply power  $P_e$  (as part of increasing the ratio  $\eta_{oe}P_e/F$ ). Increasing  $M$  as a consequence of a larger electrical supply power results in higher cable capacities, but overall system costs are only reduced as long as the costs of cable and deployment still make up a significant fraction of the overall system cost [cf. Figs. 3(e) and (f)]. Once these cost components are amortized, further increasing the spatial multiplicity of the cable is no longer cost-beneficial. Therefore, the optimum cost/bit curves reach a floor in Fig. 8, which makes work on higher electrical power supply systems of questionable impact in reducing the costs of submarine systems. For example, doubling the available optical power from  $\eta_{oe}P_e/F = 52$  dBm to  $\eta_{oe}P_e/F = 55$  dBm by significantly increasing the differential supply voltage from 30 kV to 42 kV yields an overall system cost/bit reduction of less than 15%.

### C. Optical Amplifier Bandwidth

Increasing the optical amplifier bandwidth provides linear capacity scaling but reduced SNR due to a decrease in the maximum available per-channel power and an increase in NLIN. As shown in Eq. (9), in the NL-limited regime the SNR term within the logarithm on the right hand side of the equation is proportional to  $1/\log(B)^{1/3}$ , indicating a relatively small SNR degradation resulting from increased NLIN while the pre-log factor of  $B$  promises a large potential capacity gain from wide-band amplifiers. In the linear regime of operation, the SNR is proportional to  $1/B$ , cf. Eq. (10), indicating a slightly smaller benefit from an increased amplifier bandwidth.

Another important observation that arises from Eq. (10) in the linear regime is that the cable capacity depends on  $M$  and  $B$  only through the product  $MB$ . Hence, degrees of freedom in the frequency domain can be traded for degrees of freedom in the spatial domain [13], [14]. This suggests that narrow-band amplifiers can be beneficial in terms of cost/bit as long as they provide a higher  $\eta_{oe}/F$  ratio and/or a lower cost that may compensate for the cost associated with increasing the number of spatial paths.

To illustrate the potential benefit of narrow-band OAs, we plot in Fig. 9 the normalized cost/bit in systems with optimized numbers of amplifiers  $N$ , as a function of the number of spatial paths  $M$ . We consider three types of OAs, cf. Table IV. The narrower the OA bandwidth, the higher is its efficiency and the lower is its cost. Efficiency gains come from the fact that optical gain equalization, based on attenuating high-gain spectral regions, is not needed as much in narrow-band OAs as it is in

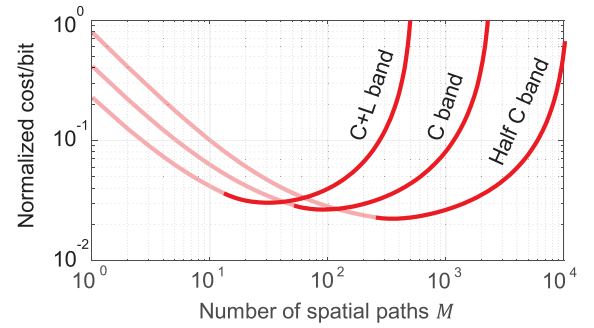


Fig. 9. Normalized cost/bit versus number of parallel paths per cable for Trans-Pacific systems using PSCF110 and different types of OAs.

TABLE IV  
COMPARISON OF DIFFERENT AMPLIFIERS FOR 11,000-KM SUBMARINE SYSTEMS USING PSCF110

	Half C band	C band	C+L band
Bandwidth $B$	18 nm	35 nm	70 nm
OA efficiency $\eta_{oe}$	6.5%	2.5%	1.3%
Noise figure $F$	5.4 dB	5 dB	5.7 dB
Normalized OA cost ( $c_{OA}$ )	0.7	2	3.6
Normalized cost/bit	0.0226	0.0268	0.0305
Optimum $M$	350	90	34
Total cable capacity $C$	4.96 Pb/s	2.37 Pb/s	1.52 Pb/s

broadband ones [13], [14]. Table IV also summarizes the normalized cost/bit in systems with optimized  $M$  and  $N$ , and the corresponding numbers of spatial paths  $M$  and cable capacities  $C$ . The narrower the OA bandwidth, the better one can scale down the cost/bit and scale up the number of spatial paths. Half C-band OAs, due to their high  $\eta_{oe}/F$  ratio and low cost, offer about 15% cost/bit savings with respect to C-band OAs, but require 350 parallel spatial paths; such systems support a huge capacity of  $\simeq 5$  Pb/s. Systems using C+L-band amplifiers, on the other hand, have  $\simeq 15\%$  higher cost/bit compared to systems using C-band OAs, but require a significantly smaller number of spatial paths and carry a much lower overall cable capacity.

## VII. SDM INTEGRATION

In all sections above we considered cost savings strictly from massive SDM using discrete state-of-the-art components in parallel, without including any cost benefits from array integration. In Fig. 10 we examine the potential benefits of amplifier and transponder integration by assuming that the overall amplifier and transponder costs are equal to  $\rho_{OA}c_{OA}NM$  and  $\rho_Tc_T C$ , where  $\rho_{OA}$  and  $\rho_T$  are the cost savings from integrating amplifiers and transponders, respectively. We plot the normalized cost/bit [Fig. 10(a)] and the corresponding number of spatial paths [Fig. 10(a)] for optimized Trans-Pacific systems as a function of these array integration cost savings. Red and blue curves, respectively, assume the array integration of amplifiers only and transponders only; black curves consider the array integration



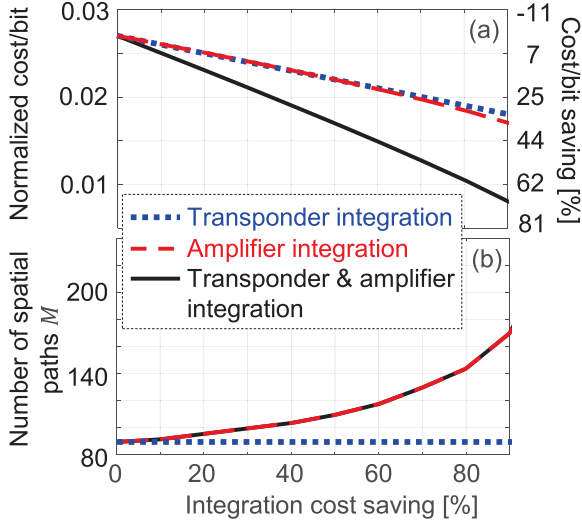


Fig. 10. Normalized cost/bit (a) and corresponding number of spatial paths (b) versus percentage of potential cost savings due to integration of transponders (blue, dotted), amplifiers (red, dashed), and both transponders and amplifiers (black, solid), assuming Trans-Pacific PSCF110 systems with optimized span lengths.

of both amplifiers and transponders, assuming the same array integration cost savings for the two. Evidently, huge savings in cost/bit can potentially be obtained from integrating amplifiers and transponders, where the benefit comes equally from amplifier and transponder array integration [as can be deduced from the similarity between the red and blue curves in Fig. 10(a)]. For instance, assuming 50% cost savings for amplifier and transponder integration results in 37% savings in the overall cost/bit of the system, totaling  $\sim 65\%$  cost/bit savings with respect to the state-of-the-art [when taking into account the 44% of cost savings from SDM without integration, as per Fig. 3(b)].

Savings from amplifier array integration would however require the installation of a higher number of spatial paths, cf. Fig. 10(b), as the lower cost of amplifiers allows for a larger number of spatial paths in amortizing the fixed cost of the cable and its deployment. As our model assumes that the cost of transponders is equal to  $\rho_T c_T C$ , the cost/bit only shifts by  $\rho_T c_T$  when assuming transponder integration at a constant cable capacity, independent of the number of spatial paths and the number of spans in the system. This explains why the blue curve in Fig. 10(b) is fixed with respect to integration savings in transponder cost.

### VIII. RELIABILITY

While massively parallelized components may reduce the overall system reliability, sufficient availability may be readily established by using a small number of additional spatial paths for protection [37]. This is visualized in Fig. 11(a), showing a submarine cable carrying the traffic of  $M/2$  WDM systems per direction on  $M/2 + mk$  spatial paths, which are selected by, e.g., an optical fail-over switch. Depending on the underlying repeater technology, the OAs within a repeater bottle may fail *independently* of each other or together in *failure groups* of  $m$  OAs.

Reliability is typically captured using *failure-in-time* (FIT) rates, whereby the probability  $P_C$  of a component failure expected to occur during any given hour of system operation is specified as  $P_C = \text{FIT} \times 10^{-9}$ , i.e., a FIT rate of 1000 corresponds to a probability of  $10^{-6}$  that a component will fail during any given hour of system operation. A system made of  $N_C$  independently failing components then fails at a probability of

$$P_S = 1 - \prod_{i=1}^{N_C} (1 - P_{C,i}) \approx \sum_{i=1}^{N_C} P_{C,i}, \quad (11)$$

where the right-hand side holds for  $P_{C,i} \ll 1$  and  $N_C$  sufficiently small. In other words, the FIT rate of a system is approximately the sum of the FIT rates of its components. A typical Trans-Pacific submarine system has a FIT rate of  $\sim 2000$  per fiber, i.e., a failure probability per spatial path of  $P_S \approx 2 \cdot 10^{-6}$ .

Consider now the case of a massively parallel submarine system whose OAs fail *independently* of each other [ $m = 1$  in Fig. 11(a)]. For  $M/2 = 50$  spatial paths per direction, the system FIT rate per direction would be as high as  $5 \times 20,000 = 100,000$ . However, adding  $k$  redundant spatial paths per direction reduces the failure probability to

$$P_{F,k} = 1 - \sum_{i=0}^k \binom{M/2 + k}{i} P_S^i (1 - P_S)^{M/2 + k - i}. \quad (12)$$

Specifically, for  $k = 0$  (no redundancy) we have

$$P_{F,0} \approx P_S M/2, \quad (13)$$

and for a single redundant path per direction ( $k = 1$ ) we have

$$P_{F,1} \approx P_S^2 \frac{M(M+2)}{8}. \quad (14)$$

More generally, if OAs fail in disjoint groups of  $m$  per repeater bottle, by adding  $k$  additional groups of  $m$  spatial paths we obtain

$$P_{F,k} \approx 1 - \sum_{i=0}^k \binom{M/2}{m} \binom{M/2 + k}{i} (m P_S)^i (1 - m P_S)^{M/2 + k - i}. \quad (15)$$

Without redundancy, this leads to the same expression as Eq. (13); adding a single group of  $m$  redundant paths per direction ( $k = 1$ ) yields

$$P_{F,1} \approx P_S^2 \frac{M(M+2m)}{8}. \quad (16)$$

Fig. 11(b) shows the results of these calculations for  $M/2 = 50$  spatial paths using no redundancy (solid), a single group of  $m$  redundant paths (dotted), and 2 groups of  $m$  redundant paths (dashed) for failure groups of  $m = 1, 5, 10, 25, 50$ . Evidently, adding a single failure group of redundant paths establishes a system FIT rate of less than  $\sim 10$ , which is well below the FIT rate of  $\sim 2000$  for an unprotected path in today's systems.

In terms of additional system cost, Fig. 12 assesses the cost of building sufficient resilience ( $k = 1$ ) into the system by adding an extra set of  $m$  optical paths per direction. Note that the costs for cable and deployment remain the same as in the unprotected system and the cost of the fail-over switch is neglected, as it will be small compared to the cost of the entire system. Protection

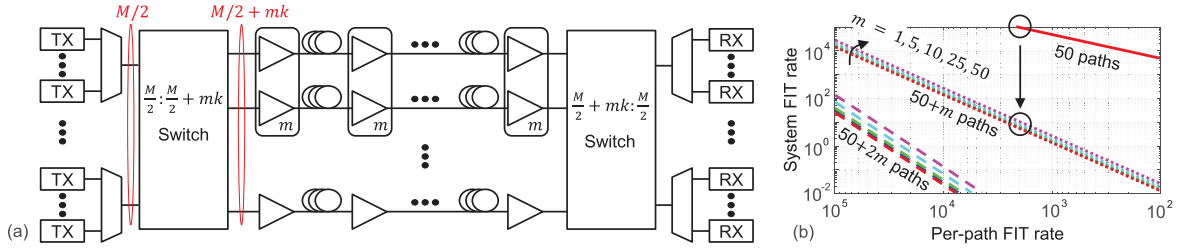


Fig. 11. (a) Illustration of a submarine cable supporting  $M/2$  WDM systems on  $M/2 + k$  spatial paths with failure groups of  $m$  OAs. (b) System FIT rate  $P_{F,k}$  versus the per-path FIT rate  $P_S$ . Solid, dotted and dashed curves correspond to systems with  $k = 0$ ,  $k = 1$  and  $k = 2$ .

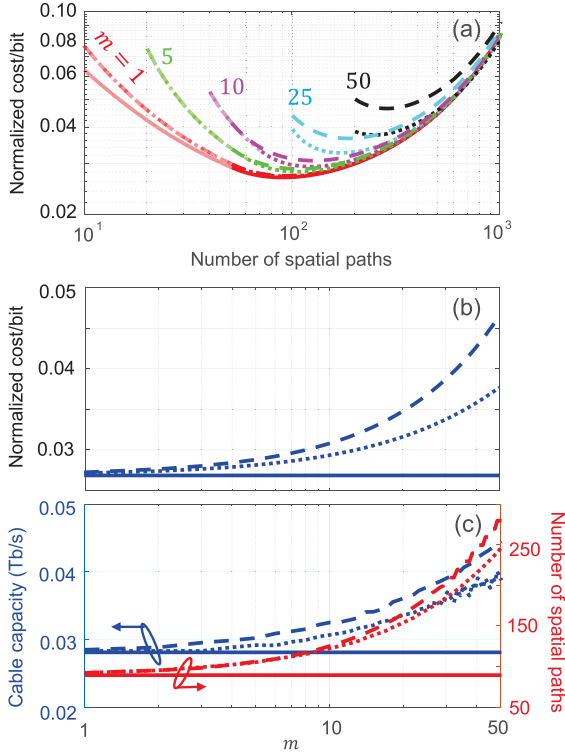


Fig. 12. (a) Normalized cost/bit versus number of spatial paths; (b) optimum normalized cost/bit; (c) corresponding cable capacity (aggregate over both directions, blue, left axis) and number of spatial paths (red, right). All versus failure group size  $m$ , for Trans-Pacific PSCF110 cables with optimized span lengths. Solid curves assume unprotected cables ( $k = 0$ ). Dotted and dashed curves assume  $k = 1$  protection with and without individual failure group power-down capabilities.

paths are not assumed to carry traffic, i.e., there are  $M$  transponders and  $M + 2mk$  parallel optical paths making up the system. Fig. 12(a) shows the normalized cost/bit as a function of the overall number of deployed spatial paths ( $M + 2m$ ). As before, light and dark coloring indicates operation in the nonlinearity-limited and power-limited regime, respectively. The red solid line represents the unprotected system ( $k = 0$ ); the dotted curves represent protected systems ( $k = 1$ ) with  $m = 1, 5, 10, 25, 50$ , for which the protection path(s) as well as the failed path(s) can be powered down, while the dashed curves assume that all working, failed, and protection paths are always powered up. It can be seen that the minimum-cost points shift to higher  $M$  as  $m$  increases, with the power-down option starting to make a

noticeable difference once the OA failure group size reaches  $\sim 10$ . These findings can be viewed as a reliability design criterion for OA arrays. Fig. 12(b) shows the minimum cost extracted from Fig. 12(a) as a function of  $m$ . The solid curve is the unprotected baseline, and the dotted and dashed curves represent systems with and without individual failure group power-down capabilities, respectively. For failure group sizes of  $\sim 10$  we find a cost increase by  $\sim 10\%$ . Fig. 12(c) shows the corresponding protected system capacities (blue, left) and overall numbers of spatial paths (red, right) versus  $m$ .

As an alternative to protecting the submarine cable as outlined above, one may also use an unprotected cable and allow  $m$ -path failure(s) at a FIT rate  $m$  times higher than the FIT rate of a single path, accepting that the affected paths will reduce the aggregate cable capacity by a fraction of  $2m/M$ , either forever or for the duration of an undersea repeater repair mission, and letting the packet layer cope with the reduced-capacity submarine pipe. Submarine repair missions are expensive and may take weeks, which makes for an interesting trade-off between the cost (or the lost value) of loosing a small fraction of cable capacity temporarily or permanently and the cost of building in protection at a premium, as discussed above.

## IX. CONCLUSIONS AND DISCUSSION

In conclusion, starting from a state-of-the-art Trans-Pacific system with 8 pairs of PSCF110 and full C-band OAs we find 44% savings for massive SDM using 45 fiber pairs based on state-of-the-art component technology. Through 50% savings from repeater and transponder integration we get another 37%, for a total cost/bit savings of 65%.

Additional aspects of our study (i) confirm the reported benefits of reduced system bandwidths, (ii) reveal the ratio of power efficiency to noise figure as a new optical amplifier figure of merit, (iii) show the reduced value of both digital nonlinearity compensation and low-nonlinearity optical fiber, (iv) and point towards massively integrated array technologies whose failure can be adequately addressed without changing the cost benefits of massive SDM submarine cables.

## APPENDIX

In its familiar version, a system's SNR is given by [24]

$$\text{SNR} = \frac{P_{ch}}{N \text{ PSD}_{\text{ASE}} B_{ch} + \chi P_{ch}^3}, \quad (17)$$

where  $P_{ch}$  is the optical signal power of a channel with bandwidth  $B_{ch}$ ,  $\text{PSD}_{\text{ASE}}$  is the power spectral density of the ASE added by one in-line amplifier, and  $\chi(B_{ch}, N_{ch})$  is the NLIN coefficient, which depends on details of the transmission system including number ( $N_{ch}$ ) and bandwidth of the WDM channels. We develop our formalism in terms of the signal's power spectral density  $\text{PSD}_{\text{sig}} = P_{ch}/B_{ch} = N_{ch}P_{ch}/B = P_{\text{tot}}/B$  and write the SNR as

$$\text{SNR} = \frac{\text{PSD}_{\text{sig}}}{N \text{PSD}_{\text{ASE}} + \chi' \log(B) \text{PSD}_{\text{sig}}^3}, \quad (18)$$

using the relationship

$$\chi P_{ch}^3/B_{ch} = \chi \text{PSD}_{\text{sig}}^3 B_{ch}^2 = \chi' \log(B) \text{PSD}_{\text{sig}}^3, \quad (19)$$

which acknowledges the fact that  $\chi(B_{ch}, N_{ch})$  scales with good accuracy as  $\chi' \log(B)/B_{ch}^2$ , with  $\chi'$ , to first order, independent of  $B$  and  $B_{ch}$  [23]–[25].

#### ACKNOWLEDGMENT

The authors gratefully acknowledge interesting and fruitful discussions with Robert W. Tkach from Nokia Bell Labs, as well as Olivier Gautheron and Olivier Courtois from Alcatel Submarine Networks (ASN).

#### REFERENCES

- [1] [Online]. Available: <https://www.wired.com/2016/05/facebook-microsoft-laying-giant-cable-across-atlantic/>
- [2] T. Frisch and S. Desbruslais, "Electrical power, a potential limit to cable capacity," in *Proc. SubOptic*, 2013, p. TU1C-4.
- [3] S. Desbruslais, "Maximizing the capacity of ultra-long haul submarine systems," in *Proc. Eur. Conf. Netw. Opt. Commun.*, 2015, pp. 1–6.
- [4] A. Pilipetskii, "High capacity submarine transmission systems," in *Proc. Opt. Commun. Fiber Conf.*, 2015, Paper W3G.5.
- [5] E. Mateo, Y. Inada, T. Ogata, S. Mikami, V. Kamalov, and V. Vusirikala, "Capacity limits of submarine cables," in *Proc. SubOptic*, 2016, Paper TH1A-1.
- [6] N. Doran and A. Ellis, "Minimizing total energy requirements in amplified links by optimising amplifier spacing," *Opt. Express*, vol. 22, pp. 19810–19817, 2014.
- [7] K. Balemarchy and R. Lingle, "Bit rate-distance product limits for uncompensated coherent multi-core fiber links under total power constraint," in *Proc. Eur. Conf. Opt. Commun.*, 2015, Paper P.5.14.
- [8] O. D. Domingues, D. A. Mello, R. da Silva, S. O. Arik, and J. M. Kahn, "Capacity limits of space-division multiplexed submarine links subject to nonlinearities and power feed constraints," in *Proc. Opt. Fiber Commun. Conf.*, 2017, Paper Th2A.50.
- [9] O. D. Domingues, D. A. Mello, R. da Silva, S. O. Arik, and J. M. Kahn, "Achievable rates of space-division multiplexed submarine links subject to nonlinearities and power feed constraints," *J. Lightw. Technol.*, vol. 35, no. 18, pp. 4004–4010, Sep. 2017.
- [10] O. V. Sinkin, A. V. Turukhin, W. W. Patterson, M. A. Bolshtyansky, D. G. Foursa, and A. N. Pilipetskii, "Maximum optical power efficiency in SDM based optical communication systems," *IEEE Photon. Technol. Lett.*, vol. 29, no. 13, pp. 1075–1077, Jul. 2017.
- [11] A. Pilipetskii, O. Sinkin, A. Turukhin, M. Bolshtyansky, and D. Foursa, "The role of SDM in future transoceanic transmission systems," in *Proc. Eur. Conf. Opt. Commun.*, 2017, Paper Tu.1.E.1.
- [12] J. Downie, "Maximum cable capacity in submarine systems with power feed constraints and implications for SDM requirements," in *Proc. Eur. Conf. Opt. Commun.*, 2017, Paper Tu.1.E.4.
- [13] A. Turukhin *et al.*, "105.1 Tb/s power-efficient transmission over 14,350 km using a 12-core fiber," in *Proc. Opt. Fiber Commun. Conf.*, 2016, Paper Th4C.1.
- [14] Y. Sun, O. V. Sinkin, A. V. Turukhin, M. A. Bolshtyansky, D. G. Foursa, and A. N. Pilipetskii, "SDM for power efficient transmission," in *Proc. Opt. Fiber Commun. Conf.*, 2017, Paper M2F.1.
- [15] R. Maher *et al.*, "Capacity approaching transmission using probabilistic shaping and DBP for PFE constrained submarine optical links," in *Proc. Eur. Conf. Opt. Commun.*, 2016, Paper M.1.D.4.
- [16] R. Dar, P. J. Winzer, A. R. Chraplyvy, S. Zsigmond, K.-Y. Huang, H. Fevrier, and S. Grubb, "Submarine cable cost reduction through massive SDM," in *Proc. Eur. Conf. Opt. Commun.*, 2017, Paper Tu.1.E.5.
- [17] M. Secondini and E. Forestieri, "Scope and limitations of the nonlinear Shannon limit," *J. Lightw. Technol.*, vol. 35, no. 4, pp. 893–902, Feb. 2017.
- [18] Y. Tang, W. Shieh, and B. S. Krongold, "DFT-spread OFDM for fiber nonlinearity mitigation," *IEEE Photon. Technol. Lett.*, vol. 22, no. 16, pp. 1250–1252, Aug. 2010.
- [19] L. B. Du and A. J. Lowery, "Optimizing the subcarrier granularity of coherent optical communications systems," *Opt. Express*, vol. 19, pp. 8079–8084, 2011.
- [20] P. Poggiolini *et al.* "Analytical and experimental results on system maximum reach increase through symbol rate optimization," *J. Lightw. Technol.*, vol. 34, no. 8, pp. 1872–1885, Apr. 2016.
- [21] R.-J. Essiambre, G. Kramer, P. J. Winzer, G. J. Foschini, and B. Goebel, "Capacity limits of optical fiber networks," *J. Lightw. Technol.*, vol. 28, no. 4, pp. 662–701, Feb. 2010.
- [22] P. Serena, "Nonlinear signal-noise interaction in optical links with nonlinear equalization," *J. Lightw. Technol.*, vol. 34, no. 6, pp. 1476–1483, Mar. 2016.
- [23] C. Xia *et al.* "Impact of channel count and PMD on polarization-multiplexed QPSK transmission," *J. Lightw. Technol.*, vol. 29, no. 21, pp. 3223–3229, Nov. 2011.
- [24] P. Poggiolini, G. Bosco, A. Carena, V. Curri, Y. Jiang, and F. Forghieri, "The GN model of fiber non-linear propagation and its applications," *J. Lightw. Technol.*, vol. 32, no. 4, pp. 694–721, Feb. 2014.
- [25] R. Dar and P. J. Winzer, "Nonlinear interference mitigation: Methods and potential gain," *J. Lightw. Technol.*, vol. 35, no. 4, pp. 903–930, Feb. 2017.
- [26] R. Dar, M. Feder, A. Mecozzi, and M. Shtaif, "Accumulation of nonlinear interference noise in fiber-optic systems," *Opt. Express*, vol. 22, pp. 14199–14211, 2014.
- [27] R. Dar, M. Feder, A. Mecozzi, and M. Shtaif, "Nonlinear Interference noise wizard," [Online]. Available: <http://nlinwizard.eng.tau.ac.il>
- [28] G. Böcherer, F. Steiner, and P. Schulte, "Bandwidth efficient and rate-matched low-density parity-check coded modulation," *IEEE Trans. Commun.*, vol. 63, no. 12, pp. 4651–4665, Dec. 2015.
- [29] F. Buchali, F. Steiner, G. Böcherer, L. Schmalen, P. Schulte, and W. Idler, "Rate adaptation and reach increase by probabilistically shaped 64-QAM: An experimental demonstration," *J. Lightw. Technol.*, vol. 34, no. 7, pp. 1599–1609, Apr. 2016.
- [30] A. Ghazisaeidi *et al.* "Advanced C + L-band transoceanic transmission systems based on probabilistically shaped PDM-64QAM," *J. Lightw. Technol.*, vol. 35, no. 7, pp. 1291–1299, Apr. 2017.
- [31] J. Cho *et al.*, "Trans-Atlantic field trial using probabilistically shaped 64-QAM at high spectral efficiencies and single-carrier real-time 250-Gb/s 16-QAM," in *Proc. Opt. Fiber Commun. Conf.*, 2017, Paper Th5B-3.
- [32] K. Takehira, "Submarine system powering," in *Undersea Fiber Communication Systems*, 2nd ed. J. Chesnoy Ed. New York, NY, USA: Academic, 2016.
- [33] X. Chen and W. Shieh, "Closed-form expressions for nonlinear transmission performance of densely spaced coherent optical OFDM systems," *Opt. Express*, vol. 18, pp. 19039–19054, 2010.
- [34] K. Saitoh and S. Matsuo, "Multicore fiber technology," *J. Lightw. Technol.*, vol. 34, no. 1, pp. 55–66, Jan. 2016.
- [35] P. W. Juodawlkis *et al.* "High-power, low-noise 1.5- $\mu$  m slab-coupled optical waveguide (SCOW) emitters: Physics, devices, and applications," *J. Sel. Topics Quantum Electron.*, vol. 17, pp. 1698–1714, 2011.
- [36] J. Renaudier *et al.*, "First 100-nm continuous-band WDM transmission system with 115Tb/s transport over 100km using novel ultra-wideband semiconductor optical amplifiers," in *Proc. Eur. Conf. Opt. Commun.*, 2017, Paper Th.PDP.A.3.
- [37] P. J. Winzer and M. Duelk, "Reliability considerations for parallel 100G carrier-grade Ethernet transport," [Online]. Available: [http://www.ieee802.org/3/hssg/public/jan07/winzer\\_01\\_0107.pdf](http://www.ieee802.org/3/hssg/public/jan07/winzer_01_0107.pdf)